

Supporting Information

Realisation and Advanced Engineering of True Optical Rugate Filters Based on Nanoporous Anodic Alumina by Sinusoidal Pulse Anodisation

Abel Santos^{1,2*}, Jeong Ha Yoo^{1,2}, Charu Vashisth Rohatgi¹, Tushar, Kumeria¹,
Ye Wang¹ and Dusan Losic^{1,2*}

¹School of Chemical Engineering, The University of Adelaide, Engineering North Building, 5005 Adelaide, Australia

²Institute for Photonics and Advanced Sensing (IPAS), The University of Adelaide, 5005 Adelaide, Australia

*E-Mails: abel.santos@adelaide.edu.au ; dusan.losic@adelaide.edu.au

S1. Summary of Results

Table S1 compiles a comprehensive summary of the experiments carried out in our study, where the effect of the main anodisation parameters on the position of the characteristic reflection peaks of NAA-RFs was systematically analysed. To this end, a NAA-RF produced with $T_p = 650$ s, $A_j = 0.420$ mA cm⁻², $J_{offset} = 0.28$ mA cm⁻², $N_p = 150$ pulses, $T_{An} = -1^\circ\text{C}$ and $t_{pw} = 0$ min was chosen as the reference structure. From this, the anodisation period (T_p), the anodisation amplitude (A_j), the anodisation offset (J_{offset}), the number of pulses (N_p), the anodisation temperature (T_{An}) and the pore widening time (t_{pw}) were systematically modified from 450 to 1400 s ($\Delta T_p = 50$ s), from 0.105 to 0.735 mA cm⁻² ($\Delta A_j = 0.105$ mA cm⁻²), from 0.14 to 0.98 mA cm⁻² ($\Delta J_{offset} = 0.14$ mA cm⁻²), from 100 to 300 pulses ($\Delta N_p = 50$ pulses), from -1 to 6°C ($\Delta T_{An} = 1^\circ\text{C}$) and from 0 to 10 min ($\Delta t_{pw} = 2$ min), respectively.

S2. Refractive Index of Aqueous Solutions of Glucose

Figure S1 shows a fitting line between the concentration of glucose and the refractive index of the solution. This relationship was used to establish a direct correlation between the level of change in λ_{peak} and the refractive index of the medium filling the nanopores of NAA-RFs.

S3. Estimation of $\Delta\lambda_{peak}$ in Real-Time by RIFS

NAA-RFs were functionalised with HSA via APTES silanization using GTA as a coupling agent. The reversible binding affinity between HSA and indomethacin molecules was assessed by measuring changes in the position of the characteristic reflection peak (1st order) of NAA-RFs in real-time by RIFS. **Figure S2** shows representative RIFS spectra from which $\Delta\lambda_{peak}$ associated with each stage of the sensing process was estimated.

Realisation and Advanced Engineering of True Optical Rugate Filters Based on Nanoporous Anodic Alumina by Sinusoidal Pulse Anodisation

Table S1. Comprehensive summary of the effect of the different anodisation parameters on the position of the characteristic reflection peaks of NAA-RFs analysed in this study.

Analysed Parameter	Range and Step Size	Peaks	Fitting Parameters	Range of λ_{Peak}
Anodisation Period - T_p	From 450 to 1400 s $\Delta T_p = 50$ s	1 st Order	$Slope = 0.67 \pm 0.01 \text{ nm s}^{-1}$ $Intercept = 130.21 \pm 13.95 \text{ nm}$ $R^2 = 0.9912$	401 – 1036 nm (Red Shift)
		2 nd Order	$Slope = 0.29 \pm 0.01 \text{ nm s}^{-1}$ $Intercept = 98.93 \pm 7.25 \text{ nm}$ $R^2 = 0.9899$	260 – 513 nm (Red Shift)
		3 rd Order	$Slope = 0.16 \pm 0.02 \text{ nm s}^{-1}$ $Intercept = 109.11 \pm 26.41 \text{ nm}$ $R^2 = 0.8537$	278 – 347 nm (Red Shift)
Anodisation Amplitude - A_j	From 0.105 to 0.735 mA cm ⁻² $\Delta A_j = 0.105 \text{ mA cm}^{-2}$	1 st Order	$Slope = 970.74 \pm 28.13 \text{ nm (mA cm}^{-2}\text{)}^{-1}$ $Intercept = 166.22 \pm 13.21 \text{ nm}$ $R^2 = 0.9950$	283 – 886 nm (Red Shift)
		2 nd Order	$Slope = 464.60 \pm 47.99 \text{ nm (mA cm}^{-2}\text{)}^{-1}$ $Intercept = 98.03 \pm 28.28 \text{ nm}$ $R^2 = 0.9687$	289 – 443 nm (Red Shift)
Anodisation Offset - J_{Offset}	From 0.14 to 0.98 mA cm ⁻² $\Delta J_{Offset} = 0.14 \text{ mA cm}^{-2}$	1 st Order	$Slope = 865.48 \pm 23.83 \text{ nm (mA cm}^{-2}\text{)}^{-1}$ $Intercept = 303.44 \pm 14.92 \text{ nm}$ $R^2 = 0.9955$	431 – 1163 nm (Red Shift)
		2 nd Order	$Slope = 435.32 \pm 24.27 \text{ nm (mA cm}^{-2}\text{)}^{-1}$ $Intercept = 152.29 \pm 16.35 \text{ nm}$ $R^2 = 0.9847$	290 – 587 nm (Red Shift)
Number of Pulses - N_p	From 100 to 300 pulses $\Delta N_p = 50$ pulses	1 st Order	$Slope = -0.97 \pm 0.11 \text{ nm pulse}^{-1}$ $Intercept = 715.37 \pm 17.27 \text{ nm}$ $R^2 = 0.9740$ NB: Fitting from 100 to 200 pulses	623 – 525 nm (Blue Shift)
		2 nd Order	$Slope = -0.54 \pm 0.03 \text{ nm pulse}^{-1}$ $Intercept = 369.50 \pm 4.63 \text{ nm}$ $R^2 = 0.9939$ NB: Fitting from 100 to 200 pulses	318 – 263 nm (Blue Shift)
Anodisation Temperature - T_{An}	From -1 to 6°C $\Delta T_{An} = 1^\circ\text{C}$	1 st Order	$Slope = -20.37 \pm 1.57 \text{ nm }^\circ\text{C}^{-1}$ $Intercept = 537.31 \pm 5.34 \text{ nm}$ $R^2 = 0.9597$	562 – 421 nm (Blue Shift)
		2 nd Order	$Slope = -5.26 \pm 0.87 \text{ nm }^\circ\text{C}^{-1}$ $Intercept = 280.57 \pm 1.06 \text{ nm}$ $R^2 = 0.9229$	286 – 270 nm (Blue Shift)
Pore Widening Time - t_{pw}	From 0 to 10 min $\Delta t_{pw} = 2$ min	1 st Order	$Slope = -15.15 \pm 1.10 \text{ nm min}^{-1}$ $Intercept = 560.40 \pm 6.67 \text{ nm}$ $R^2 = 0.9741$	563 – 401 nm (Blue Shift)
		2 nd Order	$Slope = -10.06 \pm \text{NA nm min}^{-1}$ $Intercept = 287.32 \pm \text{NA nm}$ $R^2 = \text{NA}$ NB: Only two points	286 – 266 nm (Blue Shift)

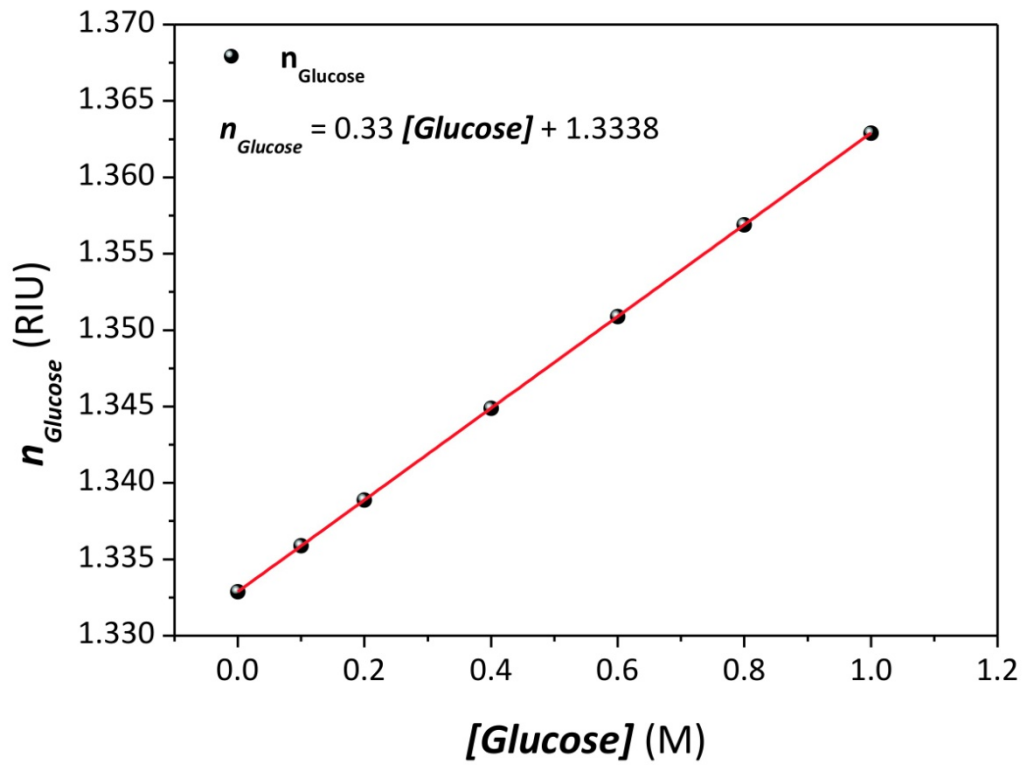


Figure S1. Estimation of the refractive index of aqueous solutions of glucose ($n_{Glucose}$) as a function of their concentration ($[Glucose]$).

Realisation and Advanced Engineering of True Optical Rugate Filters Based on Nanoporous Anodic Alumina by Sinusoidal Pulse Anodisation

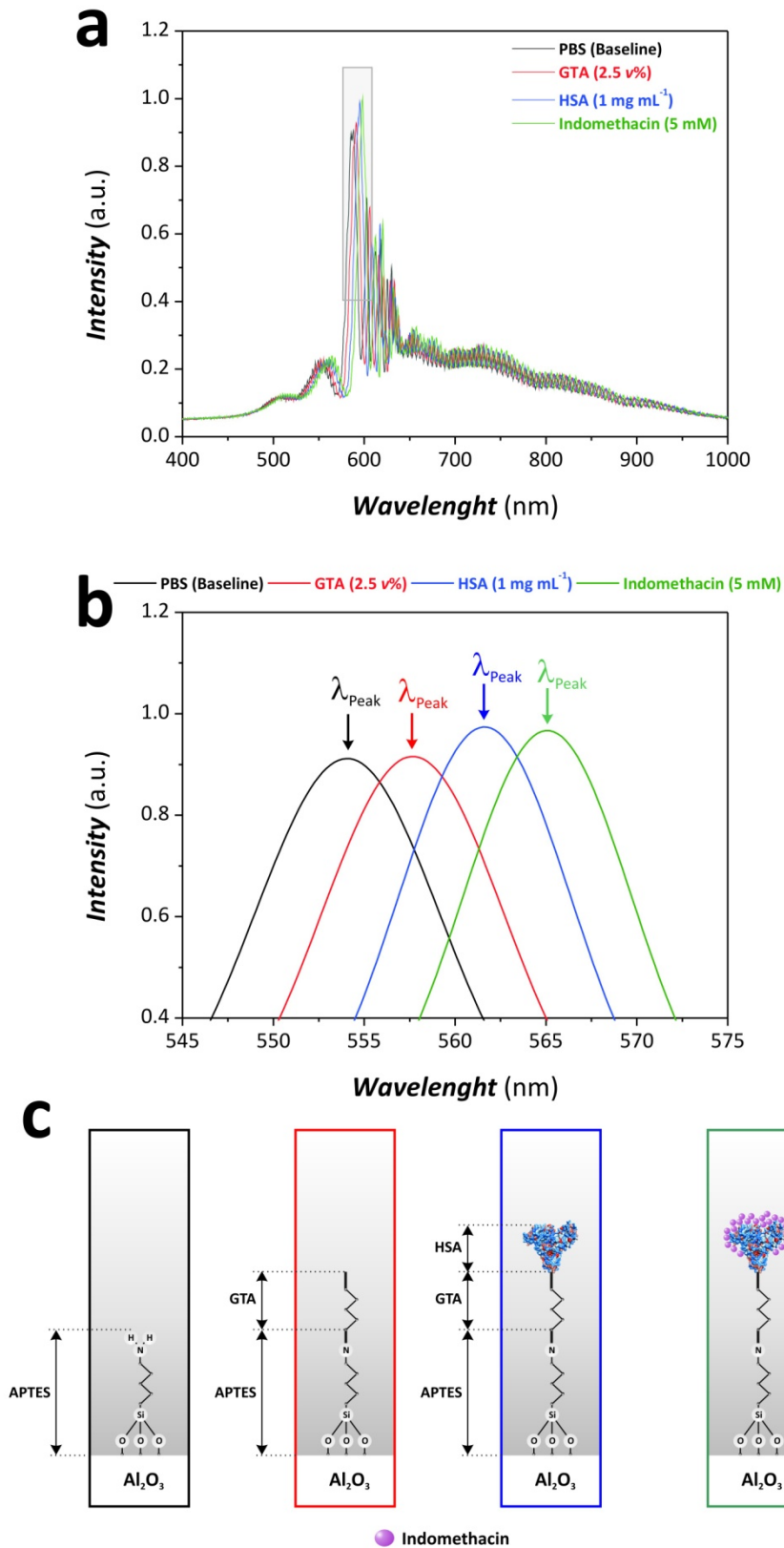


Figure S2. Example of estimation of changes in the characteristic reflection peak position (λ_{Peak}) for the assessment of the interaction between HSA molecules and indomethacin by combining APTES-functionalised NAA-RFs and RfS. a) General RfS spectra of a NAA-RFs at each stage of the sensing process. b) Magnified view of the 1st order reflection peak shown in (b) (grey rectangle). c) Schematic illustration showing the different stages of the sensing process.